Vietnam Journal of Biotechnology **23**(2): 227-238, 2025. DOI: 10.15625/vjbt-22299

GENOMIC CHARACTERIZATION AND MOLECULAR DOCKING IDENTIFIED A COPPER AMINE OXIDASE INVOLVED IN HUPERZINE A BIOSYNTHESIS IN ENDOPHYTIC FUNGI *Daldinia* SP. TLC19

Thuy Phuong Do[1], Khac Hung Nguyen[1,2], Thi Minh Thanh Le[1], Thi Thoan Pham[1] and Bich Ngoc Pham[1,3,✉]

[1]*Institute of Biotechnology, Vietnam Academy of Science and Technology, 18 Hoang Quoc Viet, Cau Giay, Hanoi, 10000, Vietnam*

[2]*Center for High Technology Research and Development, Vietnam Academy of Science and Technology, 18 Hoang Quoc Viet, Cau Giay, Hanoi, 10000, Vietnam*

[3]*Graduate University of Science and Technology, Vietnam Academy of Science and Technology, 18 Hoang Quoc Viet, Cau Giay, Hanoi, 10000, Vietnam*

✉To whom correspondence should be addressed. Email: pbngoc@ibt.ac.vn

Received: 16.01.2025
Accepted: 26.03.2025

ABSTRACT

Huperzine A (HupA), a lycopodium alkaloid derived from several species of the Huperzia family and some filamentous fungi, has been studied intensively for decades due to its reversible inhibition of acetylcholinesterase and enhanced cognitive function. In our previous study, nine HupA producing endophytic fungi were isolated from *Huperzia javanica*, including high yield species *Daldinia* sp. TLC19 with a HupA concentration of approximately 0.305 mg/g dry cellular weight (dcw). In order to determine the essential genes involved in the HupA biosynthesis pathway in *Daldinia* sp. TLC19, the whole genome sequencing was performed. Reads were assembled following the Hierarchical Genome Assembly Process (HGAP) method. The genome size was 41 MB and the GC content was about 48.2%. BUSCO analysis revealed high-quality assembly with a completeness score of approximately 98.5% and the repetitive gene ratio of around 0.1%. A putative copper amine oxidase (CAO), which catalyzes the transformation of cadaverine to 5-aminopentanal in the HupA biosynthesis pathway, was determined based on genome annotation with GenBank, the protein domain database and protein secondary structure mapping. In the molecular docking analysis, the binding of cadaverine to topaquinone (autocatalytic oxidation of tyrosine residue 415) at the active site supported the determination of *Daldinia* sp. TLC19 copper amine oxidase. Our finding on the copper amine oxidase encoding gene of endophytic fungi TLC19 could be used in further research on high HupA producing strain improvement.

Keywords: copper amine oxidase, *Daldinia* sp. TLC19, endophytic fungi, genome annotation, Huperzine A biosynthesis pathway, molecular docking

INTRODUCTION

Dementia is a neurodegenerative clinical syndrome characterized by cognitive impairment, and Alzheimer's disease (AD) is the leading cause of dementia worldwide. AD is a progressive disease characterized by individuals experiencing neuronal damage that severely affects the fundamental brain functions like storing memory, daily behavior, and language processing (Rahman *et al.*, 2024). Especially, AD patients have a low level of acetylcholine, an important neurotransmitter, which can be broken-down into acetate and choline by acetylcholinesterase (AchE). Acetylcholinesterase inhibitors (AChEI), like Tacrine (Crismon, 1994), Donepezil (Marucci *et al.*, 2020), and Rivastigmine (Birks *et al.*, 2015), block or reduce the breakdown of acetylcholine and increase the availability of acetylcholine. Several studies have demonstrated that Huperzine A is a potent, selective, and reversible AChEI for treating AD and other memory-impairment-related diseases (Marucci *et al.*, 2021; H. Zhang, 2012).

Huperzine A (HupA) is a lycopodium alkaloid derived from the medicinal plant *Huperzia serrata* (Lycopodiaceae family). Even though *H. serrata* is the primary source of HupA, the content of the compound is low in dry herb, around 0.025% (H. Zhang, 2012). Its yields had been recorded in Da Lat, Viet Nam in spring and summer at 0.0754 mg/g dw and 0.0925 mg/g dw respectively (Ngoc *et al.*, 2016). Endophytic fungi are readily manipulable due to their simple genome, making them a promising alternative source for HupA. A systematic review revealed that 32 endophytic fungal strains from 15 genera, such as *Aspergillus*, *Trichoderma*, *Coniochaeta*, *Rhizoctonia*, *Alternaria*, *Plectosphaerella*, *Podospora*, *Penicillium*, *Cyphellophora*, *Colletotrichum*, *Acremonium*, *Blastomyces*, and *Botrytis*, have been recorded for their ability to synthesize HupA, highlighting potential alternative sources for the production of this valuable compound (Ariantari & Putri, 2023; Le *et al.*, 2023; Marucci *et al.*, 2021; Thi Minh Le *et al.*, 2019).

Thi Minh Le *et al.*, 2019 successfully isolated a high yielded HupA endophyte fungus *Daldinia* sp. TLC19 from *H. javaniva,* with the average yield approximately 0.305 mg/g dcw. This significantly surpasses the previously reported yields, such as *Shiraia* sp. Slf14 with 0.1426 mg/g dcw (Zhu *et al.*, 2010) and *Cladosporium cladosporioides* ES026 with 0.045 mg/g dcw (Z. B. Zhang *et al.*, 2011). *Daldinia* was reported to be isolated from *H. serrata* for the first time in 2010 (Chen *et al.*, 2011) and Thi Minh Le *et al.*, 2019 revealed that it produces HupA for the first time in Vietnam. However, the study was only focused on *Daldinia* sp. TLC19 morphology, molecular phylogeny and HupA production (Thi Minh Le *et al.*, 2019), there is no further study focused on the fungus genome. The complete biosynthetic pathway of HupA remains unclear. However, based on the chemical synthesis of lycopodium alkaloids, Ma and Gang proposed a biosynthetic pathway for HupA (Ma & Gang, 2004). The biosynthesis of HupA includes primary and secondary metabolites. Primary metabolism begins with acetyl-CoA and biotin and ends with the formation of L-lysine, while secondary metabolism starts with the production of cadaverine (Figure 1) (G. Zhang *et al.*, 2015; Li *et al.*, 2022).

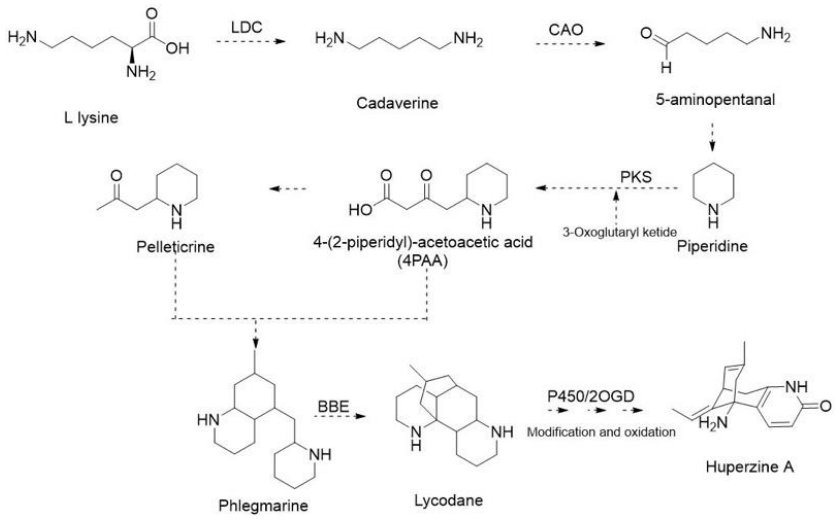

Figure 1. The proposed biosynthetic pathway of HupA. LDC, lysine decarboxylase; CAO, copper amine oxidase; PKS, polyketide synthase; BBE, berberine bridge enzyme (Li *et al.*, 2022).

One of the key enzymes in the catalytic pathway is copper amine oxidase (CAO). The CAOs are homodimers with each unit being about 70-80 kDa. Cu^{2+} and 2,4,5-trihydoxyphenylalanine quinone, or topaquinone (TPQ) cofactors are required at the active site of each subunit for activity. The CAO catalyzes the primary amine cadaverine to produce aldehyde (5-aminopentanal), ammonia, and hydrogen peroxide (H_2O_2). TPQ is a protein-derived redox factor modified from the tyrosine side chain with the presence of copper and oxygen. The modified tyrosine residue (Y) is in the active motif TXXNYE for substrate binding, with the tyrosine being the key catalytic base. The conserved HXH motif is known as the copper binding active site (Parsons *et al.*, 1995). Upon entering the active site, cadaverine undergoes deprotonation, which is facilitated by a conserved aspartate residue that acts as a general base. TPQ residue can exist in two conformations: an "off-copper" conformation and an "on-copper" conformation. The "off-copper" conformation is the catalysis conformation, while the "on-copper" conformation is less favorable for substrate binding. In the productive off-copper state, cadaverine directly interacts with the C5 atom of TPQ (Nagakubo *et al.*, 2019), leading to the substrate oxidation of cadaverine into 5-aminopentanal, while reducing molecular oxygen to H_2O_2. The biosynthesis of TPQ is crucial in facilitating electron transfer and ensuring the efficient substrate conversion. The gene expression of CAO has been proved to have a positive correlation with the synthesis of HupA, stressing the importance of the enzyme in regulating the biosynthesis pathway and the potential in optimizing the biosynthesis of the compound in industrial applications (Yang *et al.*, 2016; X. Zhang *et al.*, 2017).

Recently, alongside the advancements in technologies, bioinformatic tools have been increasingly explored and applied across various researches, especially notable in studies on medicinal plant (Hoa *et al.*, 2023) and viral epitopes (Thai *et al.*, 2023; Xuan Cuong *et al.*, 2023). In addition, in this study, the genome of *Daldinia* sp. TLC19 was first

analyzed to identify genes involved in the HupA biosynthesis pathway. Based on the genome analysis results, the key gene implicated in the biosynthesis pathway was further tested using molecular docking to predict the protein function.

MATERIALS AND METHODS

Genome sequencing, assembly, quality assessment and annotation

The *Daldinia* sp. TLC19 genome sequencing data was received from the project "Exploiting the compound Huperzine from endophytic fungi of indigenous medicinal plants of the pine family" code TĐCNSH.04/20-22. Reads were assembled by using HGAP version 4.0. Assembly quality was validated using QUAST version 4.6.3 (Mikheenko *et al.*, 2016) and BUSCO version 3 (Simão *et al.*, 2015). RepeatMasker (Flynn *et al.*, 2019) was used to identify and mask the repetitive elements in the genome. MAKER (Cantarel *et al.*, 2008) was used for gene annotation. BRAKER2 with Augustus (Brůna *et al.*, 2021) was also used without a reference genome.

For functional annotation, various databases were used for gene prediction and genome annotation. EggNOG-Mapper version 2 (Cantalapiedra *et al.*, 2021) was used to classify genes based on the Cluster of Orthologous Groups (COG), Gene Ontology (GO), and Kyoto Encyclopedia of Genes and Genomes (KEGG) databases. Additionally, similarity searches against the NCBI RefSeq and UniProtKB databases were conducted using DIAMOND version 2.0.14 (Buchfink *et al.*, 2021) to categorize predicted genes.

Identification of CAO encoding genes associated with the HupA biosynthesis pathway

Firstly, a reference sequence of CAO protein from the fungus *Colletotrichum gloeosporioides* (Accession: ALM02368) was used for finding similar sequences in *Daldinia* sp. TLC19 predicted protein database by using the BlastP tool with the e-value threshold set to 1e-05. Observed sequences were aligned with CAO protein from other species such as *Colletotrichum gloeosporioides* (Accession: ALM02368), *Shiraia* sp. Slf14 (Accession: AMB21217), *Pichia angusta* (PDB ID: 3LOY) and *Escherichia coli* (PDB ID: 1OAC) by using ClustalW (Madeira *et al.*, 2024). Subsequently, the protein domains, binding motifs and secondary structure were further analyzed with the Pfam database version 33.1 (Mistry *et al.*, 2021) and the protein secondary structure mapping tool ESPript 3 (Robert & Gouet, 2014).

Homology modeling and protein structure modification

Homology modeling was performed using SWISS-MODEL (Waterhouse *et al.*, 2018). The amino acid sequences were used to construct a protein template and the template with the highest sequence similarity was selected for protein modeling. The topaquinone residue was isolated from the CAO structure of *Hansenula polymorpha* (PDB ID: 3LOY). In the modeling structure, the tyrosine residue at position 415 was removed. Using the ChimeraX build model tool (Pettersen *et al.*, 2021), the TPQ residue model was joined to the protein structure with the removed tyrosine via a peptide bond. Before docking, the protein's energy was minimized. The structure was then prepared for docking by completing steps such as identifying and repairing missing residues, adding hydrogen atoms, and adjusting the molecular charge.

Preparation of binding substrate

Cadaverine was used as the binding substrate for molecular docking. The cadaverine structure (compound CID: 273) was retrieved from the PubChem database for chemical molecules (Kim *et al.*, 2023). The OpenBabel chemical toolbox (O'Boyle *et al.*, 2011) was used to convert the substrate format. The substrate's structure was prepared by adding hydrogen atoms and adjusting the molecular charge before docking with ChimeraX.

Molecular docking

The cadaverine structure was added to the prepared protein structure. The docking process was performed using ChimeraX with the Autodock Vina docking algorithm. Protein plus server was used to predict the binding pocket (Schöning-Stierand *et al.*, 2020). The grid box was set in the domain containing the conserved binding motif for the substrate, with the size [48.3701, 20.8313, 70.2869] and the center [-6.85714, -1.17246, 4.05034]. The other settings of the docking process were set up as default including predicted poses number: 9 poses, exhaustiveness value: 8, and maximum energy difference: 2 kcal/mol. The results were analyzed and visualized using ChimeraX and BIOVIA Discovery Studio Visualizer.

RESULTS AND DISCUSSION

Sequencing and genome annotation

The genome was deposited in public genome databases with the accession number OM943903.1. The genome size was about 41 Mb with GC content approximately 48.2%. The genome assembly was shown to be highly contiguous with the N50 of 194656 bp. The Benchmarking Universal Single-Copy Orthologs (BUSCO) analysis showed a completeness of 98.5%, demonstrating a highly complete genome assembly (Table 1).

Table 1. The genome features and assembly statistics of *Daldinia* sp. TLC19.

Genome assembly			
Total assembly size (bp)	41.101.545	Total predicted genes	13.848
Number contigs	1.782	Number of mRNAs	13.648
GC-content (%)	48.2	Complete CDS	13.322
N50 (bp)	194.656	Overlapping genes	0
L50	67	Contained genes	0
BUSCO analysis			
Completeness (%)	98.5	Fragmented BUSCOs (%)	0.3
Complete and single-copy BUSCOs (%)	98.4	Missing BUSCOs (%)	1.2
Complete and duplicated BUSCOs (%)	0.1		

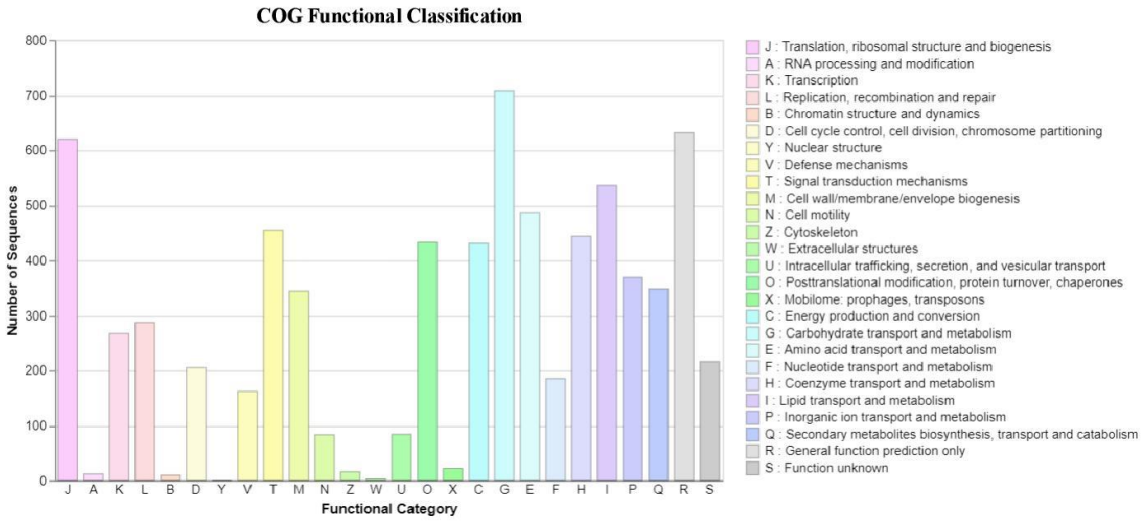

Figure 2. The functional classification of COG.

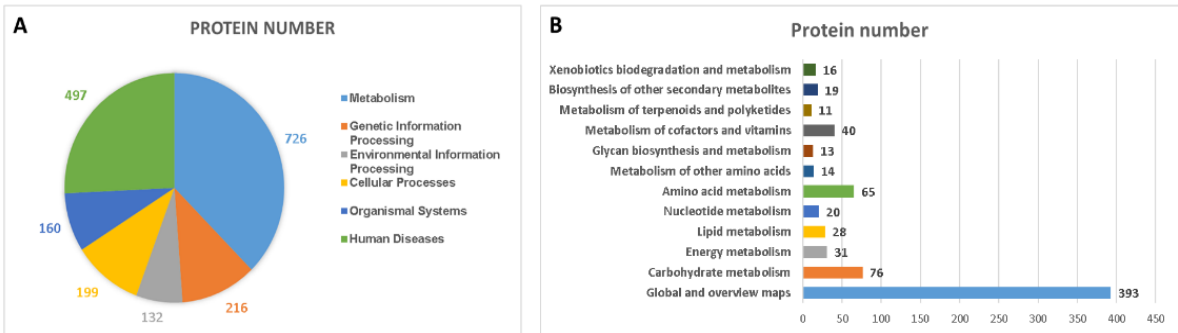

Figure 3. Annotation results with KEGG database. Overview of protein function (A) and metabolism involved protein (B).

Cluster of Orthologous Groups of proteins (COG) analysis showed that about 7,143 protein sequences (53.62%) were assigned to 26 COG categories (Figure 2). Carbohydrate transport and metabolism was the most abundant class with 708 sequences, accounting for about 9.62% of predicted proteins. Following the KEGG database analysis, about 726 proteins were predicted to be involved in the metabolism process (Figure 3). Predicted protein sequences were used for determining essential genes of the HupA biosynthesis pathway in *Daldinia* sp. TLC19.

The identification of copper amine oxidase involved in HupA synthesis in Daldinia sp. TLC19

By using BlastP against the NCBI database and performing sequence analysis, two CAO encoding genes were determined (S19_01 and S19_02) with the identity percentage (26.036 and 26.504%, respectively), and the E-value (1.80e-51 and 5.69e-57, respectively). Sequence alignment with references resulted in moderate similarity percentages that varied from 34.95 to 42.92%. Although both *Daldinia* sp. TLC19 CAO contain all of the secondary structure (alpha helix and beta sheet) in comparison

with references, functional domain analysis showed that only the S19_01 contains all of the essential domains and binding motifs of a typical copper amine oxidase. Meanwhile, the S19_02 sequence lacked copper binding site (Figure 4, Figure 5A). Previous studies showed that the CAO family had quite low sequence identity in general but the functional domains and binding motifs of substrates and copper ions were highly conserved across species (Parsons *et al.*, 1995). Therefore, *Daldinia* sp. TLC19 CAO S19_01 was used for homology modeling and protein structure modification.

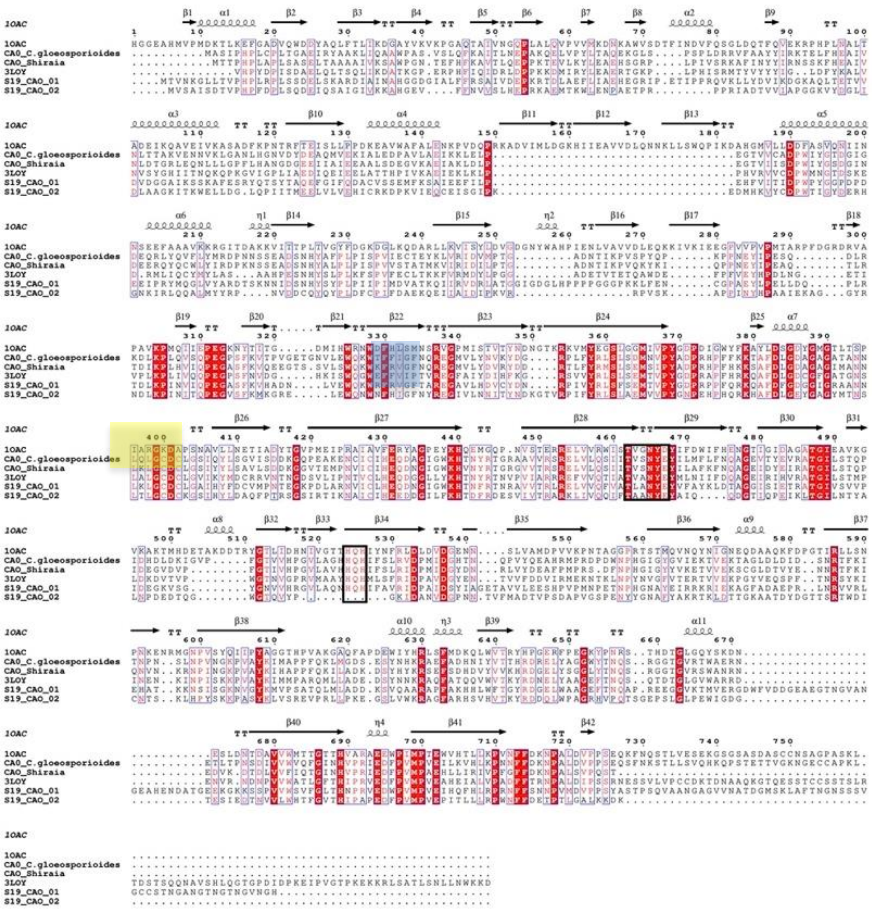

Figure 4. The alignment results and secondary structure comparison between CAO sequences. The substrate binding motif TXXNYE in blue shading and the HXH copper binding motif in yellow shading.

The global model quality estimation (GMQE score: 0.88) and the Ramachandran plot with all residues in the favored and allowed regions confirmed a good modeling process of S19_01 CAO (Figures 5A and 5B). The tyrosine residue 415 was then modified to form active TPQ for substrate binding. The RMSA score of 0.86 angstroms proves that the modified residue stayed at the exact position compared with the crystalized structure, and the modification did not cause a major conformational change that can affect the protein function (Figure 5C). TPQ modified S19_01 3D structure was used for molecular docking analysis after the energy minimization step.

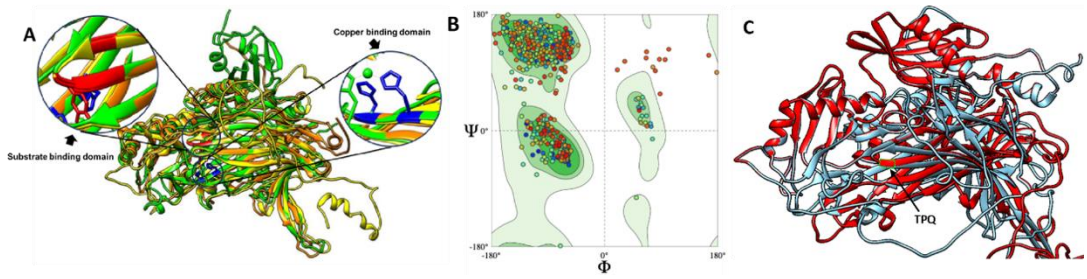

Figure 5. *Daldinia* sp. TLC19 CAOs 3D modeling aligned with reference structure (A), Ramachandran plot of CAO S19_01 3D modeling (B) and TPQ modified S19_01 3D structure (C) Green color: the reference CAO structure PDB ID: 1OAC; yellow color: CAO S19_01; orange color: CAO S19_02; Red color: CAO crystallized structure; blue color: predicted structure with modified TPQ residue; the highlighted green box: successful modified tyrosine residue.

Molecular docking predicted the binding mode of cadaverine

During the binding interaction, cadaverine must approach the C5 atom of the TPQ residue closely enough to facilitate the nucleophilic attack. A distance greater than 3 angstroms indicated the less favorable interaction, reducing the likelihood of effective catalysis. A distance of approximately 2.5 angstroms or less was considered optimal and essential for the enzyme's catalytic activity (Torrance *et al.*, 2007). Among the predicted binding poses, the most potential conformations of cadaverine expressed non-bond interactions with the C5 atom of TPQ and had the binding affinity of approximately -3.8 kcal/mol (Figure 6A).

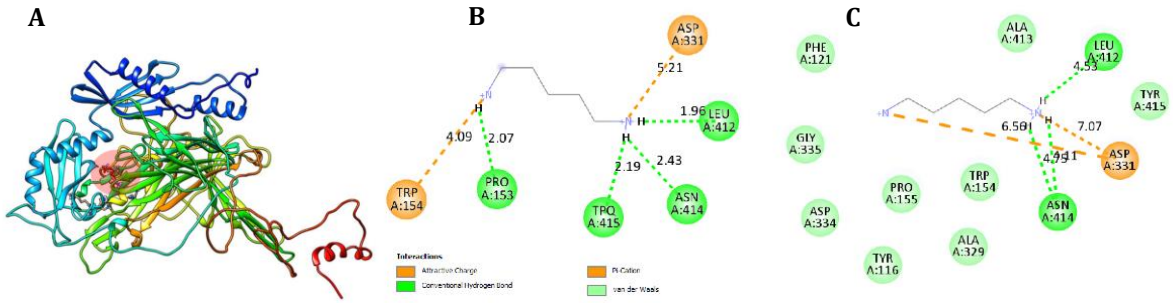

Figure 6. The molecular docking result of cadaverine and the predicted CAO (A), The 2D interaction map of the best binding conformation of cadaverine to the *Daldinia sp.* TLC19 CAO with and without TPQ modified (B) and (C). Red circle: predicted binding pocket; white ligand: predicted ligand poses; red ligand: the best binding pose.

Non-bond interaction analysis showed cadaverine exhibited electrostatic interaction with conserved aspartate residue (ASP 331) and hydrogen bond with TPQ at residue 415. Besides, several amino acids structured the cavity pocket (PRO 153, LEU 412, ASN 414 and TRP 154) and also showed interaction with cadaverine through conventional hydrogen bonds and cation-π interactions (Figure 6B). Without TPQ modified, cadaverine bound to the cavity pocket at the substrate binding site with the binding affinity at -3.5kcal/mol. Especially, the substrate only expressed weak Van der

Waals interaction with TYR 415 together with electrostatic interaction with ASP 331 and hydrogen bonds with ASN 414, LEU 412 (Figure 6C). These results once again highlight the importance of the post-translation process from tyrosine to TPQ in the function of copper amine oxidase. Without the modification, the substrate only showed weak interaction at a far distance that was insufficient for activating the catalysis.

CONCLUSION

Whole genome sequencing in combination with protein structure analysis allowed to determine two putative copper amine oxidases in the endophyte *Daldinia* sp. TLC19 genome. Amongst, the amino acid sequences of *Daldinia* sp. TLC19 CAO S19_01 contain all of the essential domains and binding motifs, ensuring the activity of enzymes such as copper ion and substrate binding domains. By using molecular docking, the binding mode of cadaverine to the protein was predicted. The substrate is strongly bound to the cavity pocket at the active site, mediated through non-bonds interacting with conserved aspartate residue (ASP 331) and TPQ at residue 415. The results also confirmed the importance of the post-translational process of changing TYR 415 to TPQ in the binding ability of cadaverine to the copper amine oxidase at the active site.

ACKNOWLEDGMENTS

This research was funded by the Vietnam Academy of Science and Technology in the projects NVCC08.02/25-25 and TĐCNSH.04/20-22.

CONFLICT OF INTEREST

The authors declare that there is no conflict of interest.

REFERENCES

Ariantari, N. P., & Putri, N. W. P. S. (2023). Production of Huperzine a by fungal endophytes associated with Huperziaceae plants. *Journal Pharmaceutical Science and Application*, *5*(1), 45–52. https://doi.org/10.24843/JPSA.2023.v05.i01.p06

Birks, J. S., Chong, L., & Grimley Evans, J. (2015). Rivastigmine for Alzheimer's disease. *The Cochrane Database of Systematic Reviews*, *2015*(9), CD001191. https://doi.org/10.1002/14651858.CD001191.pub4

Brůna, T., Hoff, K. J., Lomsadze, A., Stanke, M., & Borodovsky, M. (2021). BRAKER2: Automatic eukaryotic genome annotation with GeneMark-EP+ and AUGUSTUS supported by a protein database. *NAR Genomics and Bioinformatics*, *3*(1), lqaa108. https://doi.org/10.1093/nargab/lqaa108

Buchfink, B., Reuter, K., & Drost, H.-G. (2021). Sensitive protein alignments at tree-of-life scale using DIAMOND. *Nature Methods*, *18*(4), 366–368. https://doi.org/10.1038/s41592-021-01101-x

Cantalapiedra, C. P., Hernández-Plaza, A., Letunic, I., Bork, P., & Huerta-Cepas, J. (2021). EggNOG-mapper v2: Functional annotation, orthology assignments, and domain prediction at the metagenomic scale. *Molecular Biology and Evolution*, *38*(12), 5825–5829. https://doi.org/10.1093/molbev/msab293

Cantarel, B. L., Korf, I., Robb, S. M. C., Parra, G., Ross, E., Moore, B., *et al* (2008). MAKER: An easy-to-use annotation pipeline designed for emerging model organism genomes. *Genome Research*, *18*(1), 188–196. https://doi.org/10.1101/gr.6743907

Chen, X. Y., Qi, Y. D., Wei, J. H., Zhang, Z., Wang, D. L., Feng, J. D., *et al* (2011). Molecular identification of endophytic fungi from medicinal plant *Huperzia serrata* based on

rDNA ITS analysis. *World Journal of Microbiology and Biotechnology*, *27*(3), 495–503. https://doi.org/10.1007/s11274-010-0480-x

Crismon, M. L. (1994). Tacrine: First drug approved for Alzheimer's disease. *The Annals of Pharmacotherapy*, *28*(6), 744–751. https://doi.org/10.1177/106002809402800612

Flynn, J. M., Hubley, R., Goubert, C., Rosen, J., Clark, A. G., Feschotte, C., *et al* (2019). RepeatModeler2: Automated genomic discovery of transposable element families. *Genomics*. https://doi.org/10.1101/856591

Hoa, T. T., Thu Giang, N., Hong Ha, N. T., Huyen, T. T., Tien Phat, D., Hoang Ha, C., … Ho Quang, T. (2023). Diversity of endophytic fungi from medicinal plants *Dysosma difformis* (Hemsl & E.H. Wilson) T.H. Wang collected in Ha Giang and Lai Chau. *Vietnam Journal of Biotechnology*, *21*(2), 365–373. https://doi.org/10.15625/1811-4989/18344

Kim, S., Chen, J., Cheng, T., Gindulyte, A., He, J., He, S., *et al* (2023). PubChem 2023 update. *Nucleic Acids Research*, *51*(D1), D1373–D1380. https://doi.org/10.1093/nar/gkac956

Le, T. T. M., Pham, H. T., Trinh, H. T. T., Tran, H. T., & Chu, H. H. (2023). Isolation and characterization of novel Huperzine-producing endophytic fungi from Lycopodiaceae species. *Journal of Fungi*, *9*(12), Article 12. https://doi.org/10.3390/jof9121134

Li, X., Li, W., Tian, P., & Tan, T. (2022). Delineating biosynthesis of Huperzine A, A plant-derived medicine for the treatment of Alzheimer's disease. *Biotechnology Advances*, *60*, 108026. https://doi.org/10.1016/j.biotechadv.2022.108026

Ma, X., & Gang, D. R. (2004). The Lycopodium alkaloids. *Natural Product Reports*, *21*(6), 752–772. https://doi.org/10.1039/B409720N

Madeira, F., Madhusoodanan, N., Lee, J., Eusebi, A., Niewielska, A., Tivey, A. R. N., *et al* (2024). The EMBL-EBI Job Dispatcher sequence analysis tools framework in 2024. *Nucleic Acids Research*, *52*(W1), W521–W525. https://doi.org/10.1093/nar/gkae241

Marucci, G., Buccioni, M., Ben, D. D., Lambertucci, C., Volpini, R., & Amenta, F. (2021). Efficacy of acetylcholinesterase inhibitors in Alzheimer's disease. *Neuropharmacology*, *190*, 108352. https://doi.org/10.1016/j.neuropharm.2020.108352

Marucci, G., Moruzzi, M., & Amenta, F. (2020). Chapter 31—Donepezil in the treatment of Alzheimer's disease. In C. R. Martin & V. R. Preedy (Eds.), *Diagnosis and Management in Dementia* (pp. 495–510). Academic Press. https://doi.org/10.1016/B978-0-12-815854-8.00031-8

Mikheenko, A., Valin, G., Prjibelski, A., Saveliev, V., & Gurevich, A. (2016). Icarus: Visualizer for de novo assembly evaluation. *Bioinformatics*, *32*(21), 3321–3323. https://doi.org/10.1093/bioinformatics/btw379

Mistry, J., Chuguransky, S., Williams, L., Qureshi, M., Salazar, G. A., Sonnhammer, E. L. L., *et al* (2021). Pfam: The protein families database in 2021. *Nucleic Acids Research*, *49*(D1), D412–D419. https://doi.org/10.1093/nar/gkaa913

Nagakubo, T., Kumano, T., Ohta, T., Hashimoto, Y., & Kobayashi, M. (2019). Copper amine oxidases catalyze the oxidative deamination and hydrolysis of cyclic imines. *Nature Communications*, *10*(1), 413. https://doi.org/10.1038/s41467-018-08280-w

Ngoc, V. T., Hanh, P. T., Anh, L. T. L., Dat, N. T., & Thuy, L. T. B. (2016). Qualification and quantification of Huperzine A from *Huperia serrata* in Da Lat, Lam Dong province. *Vietnam Journal of Biotechnology*, *14*(3), 473–478. https://doi.org/10.15625/1811-4989/14/3/9861

O'Boyle, N. M., Banck, M., James, C. A., Morley, C., Vandermeersch, T., & Hutchison, G. R. (2011). Open Babel: An open chemical toolbox. *Journal of Cheminformatics*, *3*(1), 33. https://doi.org/10.1186/1758-2946-3-33

Parsons, M. R., Convery, M. A., Wilmot, C. M., Yadav, K. D. S., Blakeley, V., Corner, A. S., Phillips *et al* (1995). Crystal structure of a quinoenzyme: Copper amine oxidase of *Escherichia coli* at 2 Å resolution. *Structure*, *3*(11), 1171–1184. https://doi.org/10.1016/S0969-2126(01)00253-2

Pettersen, E. F., Goddard, T. D., Huang, C. C., Meng, E. C., Couch, G. S., Croll, T. I., *et al* (2021). UCSF ChimeraX: Structure visualization for researchers, educators, and developers. *Protein Science: A Publication of the Protein Society*, *30*(1), 70–82. https://doi.org/10.1002/pro.3943

Rahman, A., Banu, Z., Rani, R., & Mehdiya, R. (2024). Unravelling Alzheimer's disease: Insights into pathophysiology, etiology, diagnostic approaches, and the promise of aducanumab, lecanemab, and donanemab. *Journal of Phytonanotechnology and Pharmaceutical Sciences 4*(3), 1-10, 2024. https://dx.doi.org/10.54085/jpps.2024.4.3.1

Robert, X., & Gouet, P. (2014). Deciphering key features in protein structures with the new ENDscript server. *Nucleic Acids Research*, *42*(W1), W320–W324. https://doi.org/10.1093/nar/gku316

Schöning-Stierand, K., Diedrich, K., Fährrolfes, R., Flachsenberg, F., Meyder, A., Nittinger, E., *et al* (2020). ProteinsPlus: Interactive analysis of protein–ligand binding interfaces. *Nucleic Acids Research*, *48*(W1), W48–W53. https://doi.org/10.1093/nar/gkaa235

Simão, F. A., Waterhouse, R. M., Ioannidis, P., Kriventseva, E. V., & Zdobnov, E. M. (2015). BUSCO: Assessing genome assembly and annotation completeness with single-copy orthologs. *Bioinformatics*, *31*(19), 3210–3212. https://doi.org/10.1093/bioinformatics/btv351

Thai, Q. K., Huynh, P., Nguyen Thi Thuong, H., & Quan, Q.-D. (2023). Investigating the impact of spike protein mutations on SARS-CoV-2 virulence in benin using network centrality and molecular docking approaches. *Vietnam Journal of Biotechnology*, *21*(2), 219–234. https://doi.org/10.15625/1811-4989/18276

Thi Minh Le, T., Thi Hong Hoang, A., Thi Bich Le, T., Thi Bich Vo, T., Van Quyen, D., & Hoang Chu, H. (2019). Isolation of endophytic fungi and screening of Huperzine A–producing fungus from *Huperzia serrata* in Vietnam. *Scientific Reports*, *9*(1), 16152. https://doi.org/10.1038/s41598-019-52481-2

Torrance, J. W., Holliday, G. L., Mitchell, J. B. O., & Thornton, J. M. (2007). The geometry of interactions between catalytic residues and their substrates. *Journal of Molecular Biology*, *369*(4), 1140–1152. https://doi.org/10.1016/j.jmb.2007.03.055

Waterhouse, A., Bertoni, M., Bienert, S., Studer, G., Tauriello, G., Gumienny, R., *et al* (2018). SWISS-MODEL: Homology modelling of protein structures and complexes. *Nucleic Acids Research*, *46*(W1), W296–W303. https://doi.org/10.1093/nar/gky427

Xuan Cuong, H., Minh Thuong, V., Nhu Binh, D., Duc Tien, D., Thuy Linh, B., & Bich Thuy, V. T. (2023). Prediction of conservative epitopes in the NS1 sequences of all four dengue virus serotypes. *Vietnam Journal of Biotechnology*, *21*(3), 443–454. https://doi.org/10.15625/1811-4989/18423

Yang, H., Peng, S., Zhang, Z., Yan, R., Wang, Y., Zhan, J., *et al* (2016). Molecular cloning, expression, and functional analysis of the *copper amine oxidase* gene in the endophytic fungus *Shiraia* sp. Slf14 from *Huperzia serrata*. *Protein Expression and Purification*, *128*, 8–13. https://doi.org/10.1016/j.pep.2016.07.013

Zhang, G., Wang, W., Zhang, X., Xia, Q., Zhao, X., Ahn, Y., *et al* (2015). *De novo* RNA sequencing and transcriptome analysis of *Colletotrichum gloeosporioides* ES026 reveal genes related to biosynthesis of Huperzine A. *PLOS ONE*, *10*(3), e0120809. https://doi.org/10.1371/journal.pone.0120809

Zhang, H. (2012). New insights into Huperzine A for the treatment of Alzheimer's disease. *Acta*

Pharmacologica Sinica, *33*(9), 1170–1175. https://doi.org/10.1038/aps.2012.128

Zhang, X., Wang, Z., Jan, S., Yang, Q., & Wang, M. (2017). Expression and functional analysis of the lysine decarboxylase and copper amine oxidase genes from the endophytic fungus *Colletotrichum gloeosporioides* ES026. *Scientific Reports*, *7*(1), 2766. https://doi.org/10.1038/s41598-017-02834-6

Zhang, Z. B., Zeng, Q. G., Yan, R. M., Wang, Y., Zou, Z. R., & Zhu, D. (2011). Endophytic fungus *Cladosporium cladosporioides* LF70 from *Huperzia serrata* produces Huperzine A. *World Journal of Microbiology and Biotechnology*, *27*(3), 479–486. https://doi.org/10.1007/s11274-010-0476-6

Zhu, D., Wang, J., Zeng, Q., Zhang, Z., & Yan, R. (2010). A novel endophytic Huperzine A–producing fungus, *Shiraia* sp. Slf14, isolated from *Huperzia serrata*. *Journal of Applied Microbiology*, *109*(4), 1469–1478. https://doi.org/10.1111/j.1365-2672.2010.04777.x